

# MODELLING CAPSULE STABILITY ACCOUNTING FOR SHAPE CHANGE

*D. Neeb<sup>(1)</sup>, P. Seltner<sup>(1)</sup>, A. Gülhan<sup>(1)</sup>, L. Ferracina<sup>(2)</sup>*

<sup>(1)</sup> German Aerospace Center (DLR), Supersonic and Hypersonic Technology Department of the Institute of Aerodynamics and Flow Technology, Linder Hoehe, 51147 Cologne, Germany, Email:

[Dominik.Neeb@dlr.de](mailto:Dominik.Neeb@dlr.de), [Patrick.Seltner@dlr.de](mailto:Patrick.Seltner@dlr.de), [Ali.Guelhan@dlr.de](mailto:Ali.Guelhan@dlr.de)

<sup>(2)</sup> ATG Europe B.V. on behalf of the European Space Agency (ESA),  
Nordwijk, Netherlands, Email:

[Luca.Ferracina@esa.int](mailto:Luca.Ferracina@esa.int)

## ABSTRACT

Earth return missions or exploration missions use mostly capsule-like shapes, which enter the atmosphere at very high velocities. Some of these missions, like sample return, do not use any parachute or other stabilizing aerodynamic or RCS devices. Therefore, the capsule stability has to be guaranteed solely by the spacecraft configuration from hypersonic conditions down to the subsonic regime at landing. This task is very challenging and requires reliable design tools. However, both experimental and numerical tools still have shortcomings in full simulation or modelling of the flight environment. Therefore, further improvement of these tools by means of complementary application is essential.

Most of the exploration missions use an ablative thermal protection system, which experiences shape changes during the hypersonic flight regime. This may lead to a change of the pressure distribution and movement of the center of gravity of the vehicle. Since the vehicle does not have control devices, it can lose its aerodynamic stability and the situation may become critical. The prediction of the Thermal Protection System (TPS) recession over the complete surface with the existing tools is not possible. Therefore, the aerodynamic design should consider it in the margin policy and the flight qualities and risk analysis need to be performed accordingly.

The ESA TRP MODSHAPE (Modelling Capsule Stability accounting for Shape Change) addresses the aforementioned challenges and this paper gives an overview of the planned activities and summarizes the main challenges and goals.

*Index Terms*— Entry, capsule, shape change, low temperature ablator, aerodynamics

## 1. INTRODUCTION

The ESA TRP MODSHAPE (Modelling Capsule Stability accounting for Shape Change) has the main goal to experimentally quantify the impact of the Outer Mould Line (OML) changes due to TPS recession on the flight qualities of capsules of potential interest to exploration missions. The

team consists of the German Aerospace Center (DLR), Fluid Gravity, Thales Alenia Space Italy and the Royal Observatory of Belgium. Experiments with models made of low temperature ablators (LTA) will be performed in the hypersonic flow regime with simultaneous in-situ recession measurements and aerodynamic stability measurements using a six-component balance. In addition, supersonic and transonic experiments will be carried out to assess the shape recession impact on supersonic and transonic flight qualities, where the capsule stability needs to be secured. These experimental efforts are accompanied by computational fluid dynamics analyses.

In the following the paper summarizes the initial analyses and focuses on the preparations for the planned experimental activities. First, the baseline configuration for the analyses is discussed. Then, the tools used during the TRP are described. Afterwards, the model and the model coating material strategy are described. This is followed by a discussion of preliminary pre-test results. Finally a summary and outlook is given.

## 2. BASELINE CONFIGURATION

To accomplish the goal of the TRP, a baseline Earth re-entry capsule (ERC) configuration was chosen based on a multitude of criteria, like e.g. static dynamic stability, aerothermodynamic aspects, availability of aerodynamic/aerothermodynamic databases and system requirements. Two different shapes were pre-selected with the

- Hayabusa probe (modified) and
- Galileo probe (Pioneer Venus).

The Hayabusa probe has a sphere-cone forebody shape with a cone angle of 45° (Figure 1). A modified version was preferred over the former standard Hayabusa (Mu-launched space-engineering satellite, MUSES-C) shape, as it is a more likely candidate for European missions. The Hayabusa shape provides an optimum solution in terms of heat fluxes, internal component accommodation, outer envelope and subsonic stability. It had been selected as a baseline for several ESA exploration studies and was the preferred shape

for e.g. MarcoPolo-R [18], and Phobos Sample Return studies (Phootprint or PhSR) [19], [12].

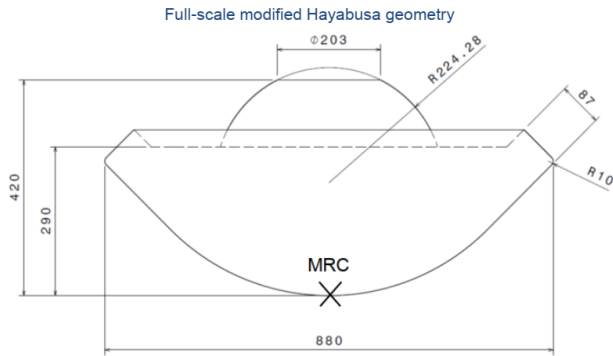


**Figure 1: Modified Hayabusa probe shape**

Besides the Hayabusa shape as main reference case, the Galileo probe shape (or sometimes called Pioneer Venus shape due to the similarities) was chosen for methodology validation [20]. Since this sphere-cone shape with a cone angle of approx.  $45^\circ$  has a smaller nose diameter, higher heat flux and therefore recession is expected.

### 3. TOOLS

The main focus of the TRP lies on the experimental quantification of shape change impacts on aerodynamic parameters. This effort is supported by numerical predictions and rebuilding. This chapter gives an overview about the used tools for both approaches. The model is described in more detail in the next chapter.

#### Experimental Tools

In order to accurately simulate flight conditions in a wind tunnel, the appropriate similarity parameters need to be duplicated as best as possible. Unfortunately, no ground-based facility is capable of fully duplicating all relevant conditions of a vehicle entering a planetary atmosphere at high-speed. Therefore, the classical approach is to duplicate the most relevant similarity parameters for the targeted load to be measured. Besides geometrical similarity, for aerodynamic measurements usually the Mach and Reynolds number of a corresponding flight trajectory point are duplicated. At high Mach numbers, the impact pressure dominates against viscous contribution for typical blunt entry vehicles. Since the shape of the bow shock has a decisive contribution and causes high temperatures, fluid chemistry need to be considered. Although some types of facilities are able to duplicate a certain region of the flight enthalpy conditions, typical short test times, very low Reynolds numbers and high uncertainties disqualify these facilities for aerodynamic purposes. Additionally, if the

vehicle is planned to enter an atmosphere other than Earth, the difference in e.g. fluid chemistry, heat capacity ratio, etc. need to be taken into account. To cover these high enthalpy effects and differences in chemistry from ground-based to flight conditions, usually CFD computations are used as bridging element. Instead of a high-enthalpy facility, it was decided to choose a cold blow-down wind tunnel providing very high accuracies for aerodynamic force measurements.

Two experimental test campaigns are planned within the TRP. First, a test campaign at hypersonic conditions will be performed with the emphasis on parallel in-situ measurements of the shape change and aerodynamic forces and moments. The second test campaign will focus on the shape change impact on aerodynamics in trans- to supersonic conditions with fixed model shapes based on the measured shape changes from hypersonic test campaign. This methodology represents the trajectory history aspect, since any shape change of the vehicle has not only an effect on the flight qualities at the flow regime where the recession occurs but also on all following conditions during the entry and descent phase.

The first test campaign will be carried out in the DLR hypersonic test section H2K. It is an intermittently working blow-down wind tunnel with a free-stream test section. Electrical heaters allow the modification of reservoir temperatures. Together with suitable reservoir pressures, stable flow conditions with Reynolds numbers between  $2.5 \cdot 10^6 \text{ m}^{-1}$  to  $20 \cdot 10^6 \text{ m}^{-1}$  can be set for test times of typically 30 seconds. The facility has contributed to several past entry missions with aerodynamic campaigns, e.g. [24], [25], [26]. The second test campaign will be performed in the DLR trisonic test section TMK. It is a blow down wind tunnel with a cross section of  $0.6 \text{ m} \times 0.6 \text{ m}$ . It is equipped with a flexible nozzle to provide a Mach number range from  $0.5 < \text{Ma} < 5.7$ .

#### Inflow conditions / scaling

FGE provided analyses of the Phobos Sample Return (PhSR) study, which used a scaled version of the Hayabusa aeroshape as ERC [12], to identify the main drivers and constraints for the tests in this TRP. The region of interest for the MODSHAPE activities wrt. recession tests (peak heating or heat pulse) falls approx. into the altitude range of 40 - 70 km, at a corresponding Mach number range of  $\text{Ma} = 5 - 35$  and Reynolds number range of  $\text{Re}_D = 0.1 \cdot 10^6 - 0.6 \cdot 10^6$ . Concerning the expected boundary layer regime in this region, the relatively low Reynolds numbers will be highly favorable for maintaining laminar flow conditions. As a further parameter the convective heat load or heat flux  $\dot{q}_c$  at the capsule stagnation point, was taken into account. It is normalized for the flight and wind tunnel conditions by the heat transported by the inflow, resulting in the Stanton

number  $St = \frac{\dot{q}_c}{\rho_\infty V_\infty (H_0 - h_w)}$ , with the inflow density  $\rho_\infty$ , the inflow velocity  $V_\infty$ , the stagnation enthalpy  $H_0$  and wall enthalpy  $h_w$ . Besides these inflow and heating parameters, the resulting force acting on the wind tunnel balance was taken into account for the inflow conditions choice. The general goal is to find a combination of flow condition, model size (capsule diameter) and force balance which ensures sufficient load factors of the balance to enable high signal-to-noise ratios and, in case of MODSHAPE, enable resolving the anticipated small changes due to shape changes.

Knowing these objectives, it is possible to investigate the options for duplication. Before one specific inflow condition was selected, a wind tunnel condition envelope was defined which encloses the parameter region of interest for preliminary numerical investigations and model coating studies as discussed in this paper (see chapter 4). Representative parameters are included in Table 1. To find a suitable inflow condition for the actual test campaign in H2K and therefore to condense to one representative inflow condition, a trade-off must be made for the duplication criteria, since they usually demand contrary requirements. For example to meet the criteria for high signal-to-noise ratios for aerodynamic measurements, sufficiently high dynamic pressures i.e. reservoir pressures are beneficial. On the contrary, the mass loss of the LTA is increasing with decreasing stagnation pressure i.e. reservoir pressure (this will be shown later in this chapter). An acceptable choice was found with a Mach 6 condition, labeled “dup” and included in Table 1. An acceptable choice for model scaling was derived with a diameter of 100mm for H2K and 80mm for TMK tests. The corresponding inflow conditions are also included in a Ma-Re-plot together with the Hayabusa sizing trajectory in Figure 2. Additionally included are the targeted flow conditions for the test campaign in TMK.

To evaluate if the requirement for a laminar boundary layer along the front shield can be accomplished in the wind tunnel, engineering transition criteria were evaluated based on boundary layer data from the calculation approach by FGE (see below). Only the maximum Reynolds number conditions were identified to show a probable tendency for transition to turbulent flow. Despite of these engineering criteria, experiences from past blunt body tests in H2K show, that even if these criteria for transition are met, it is typically very tough to realize transition along comparable blunt body surfaces. To support this estimation, additionally, an un-deformed Hayabusa shape capsule will be built from polyether ether ketone (PEEK) which is the standard material for IR thermography in H2K. Together with an in-house tool to extract the convective heat flux from the surface temperatures, the data can be compared to laminar

and turbulent computations along the front shield to identify the boundary layer state at the targeted inflow conditions.

**Table 1: Preliminary H2K wind tunnel conditions envelope**

	Mach	p <sub>0</sub> [bar]	T <sub>0</sub> [K]	Re <sub>∞</sub> [10 <sup>6</sup> ·1/m]
min	5.27	3	600	2.52
max	5.32	12	390	18.76
min	5.98	4	590	2.53
max	6.06	24	480	20.02
min	7.01	4	450	2.52
max	7.12	39	620	14.61
min	8.57	10	700	1.89
max	8.79	40	750	6.36
min	11.2	17	700	1.52
max	11.2	40	820	2.82
dup	6.01	11.3	700	5.5

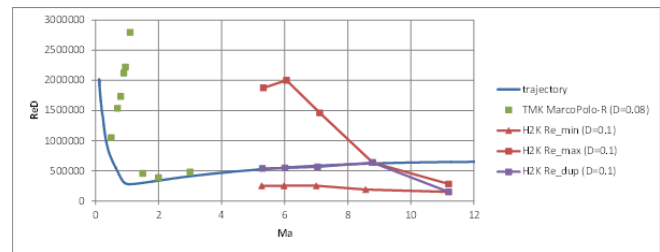


**Figure 2: Ma-Re-plot for the H2K and TMK inflow envelope**

Another important aspect from the PhSR study is the dominance of the aerodynamic frequency over the roll rate in the hypersonic trajectory phase of the Hayabusa Earth entry. Therefore, the capsule tends to a ‘Lunar motion’. With this motion, one ray of the capsule front shield tends to always face the velocity vector. Therefore, an asymmetrical shape change is possible and will be investigated with non-zero angle of attack runs during tests. A maximum of approx. 10° angle of attack is foreseen.

### Aerodynamic 6-component balances

To measure the aerodynamic forces and moments, an internal six-component moment-type force balance will be used. It is a DLR in-house design which has several strain gauges applied at well-defined positions to rebuild all three force components as well as moments. A balance was chosen from the portfolio, which is able to serve the needs for the typical load case of the blunt capsule geometries, like high axial- and low normal-/roll-loads. Numerical support

for a wind tunnel aerodynamic database was provided by SENER [13].

### Surface and recession measurements

The main goal is to perform in-situ temporally resolved recession measurements during the hypersonic tests. To check and complement these measurements, two different pre- and post-test reference surface measurements are planned. First, a tactile technique with a high precision Carl Zeiss Prismo MP5/VAST system can be used, enabling typical resolutions of  $0.2 \mu\text{m}$  and an uncertainty of  $1.5 \mu\text{m}$ . It was already applied for the model manufacturing characterization (see next chapter). A further pre- and post-test reference surface measurement will be performed by an optical 3D-profilometer (Keyence VR-5200). It has a resolution of  $0.1 \mu\text{m}$  with an uncertainty of  $4.0 \mu\text{m}$ .

The challenge for the application of an in-situ surface measurement for this study is to record a surface which not only changes its shape during time but also the upper surface is recessed and either melts or evaporates. To evaluate the expected amount of surface changes during test time, FGE provided estimations of the stagnation point recession rates under a possible H2K inflow condition envelope.

Several different approaches for in-situ surface measurements from past investigations were identified and analyzed, with the focus on non-intrusive, optical measurement techniques, i.e. [1] [2] [3] [5]. Two different approaches were chosen for an application within the current TRP, i.e. a technique based on Schlieren images and a photogrammetric approach.

Schlieren optics systems exploit the effect of density gradients on the light propagation through a flow field. This setup is typically used to observe shock waves or expansion regions in the flow field. Since the contour of a model within the flow field is captured as well, the images can be used to track a change of the shape. Due to the imaging technique, only the contour for the line of sight of the model is visible and therefore the measured shape change is typically restricted to the symmetry plane of the model (see also Figure 9, a).

The chosen photogrammetric approach is called Projected Texture Stereo Vision (PTSV) [15]. The measuring system consists of a projector and two cameras. A specific pattern is typically projected by a suitable light source in combination with a suitable optics by the projector onto the object of interest (see Figure 3, a). The object with patterns along its surface is recorded by the cameras, whereby two cameras are incorporated in case of a stereo vision system. With the help of a suitable camera calibration, 3D points can be rebuilt by the stereo system. The pattern consists of a random arrangement of dark rectangles, where the light

from the projector is blocked. An example of such a pattern recorded by one of the stereo cameras is visible in Figure 3, b.

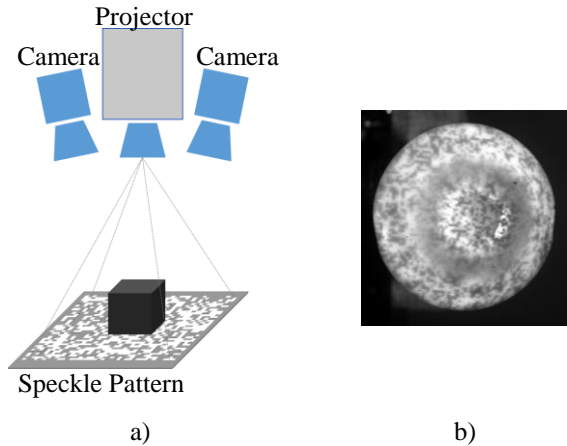


**Figure 3: Schematic set-up of PTSV after [27] a), an example raw image b)**

The PTSV set-up with the LED pattern projector enables higher resolution than a laser dot based system, since it is defined by a combination of the amount of pattern and camera pixels ([15]) instead of the amount of laser dots ([3]). The example set-up visualized in Figure 3, b resulted in approx. 7000 points along the surface of the capsule front shield. Another aspect which was considered is that the laser refraction optics is typically much more expensive. A test set-up was installed outside of the H2K test section to characterize the rebuilding of the capsule surface. The projector and camera positions as well as the distance to the model were chosen to be representative for a typical set-up in the H2K test section. Both, models with wax and camphor coating were tested (see also next section). As reference, tactile profile measurements along the front shield model coating were performed with the high precision Carl Zeiss Prismo MP5/VAST. The more challenging coating is the camphor coating due to its optical characteristics. Model regions, where the camphor has a partly milky white opaque appearance, show good reflective characteristics and PTSV results show typical rms deviations in the order of approx. 0.1mm in the nose and approx. 0.2mm along the cone region. Some regions show higher deviations. This can mainly be attributed to material properties, since in these regions the coating consists of a clear, translucent mass, which has inferior reflective characteristics (see also Figure 3, b). A check will be made on the impact of the effect under the wind tunnel test conditions.

Additionally, infrared thermography (IR) camera measurements are planned to capture the surface temperatures during the test runs.

#### Numerical tools

The numerical prediction of forces and moments on the wind tunnel model is performed by SENER applying STAR-CCM+ to solve the RANS equations [13]. The results were used to guide the choice of aerodynamic force balance in both targeted wind tunnel campaigns.

The preliminary prediction of recession rates as well as the post-test rebuilding of the hypersonic recession tests and its impact on the aerodynamic forces is performed by FGE applying their Shape-changing Module Code for Hypersonics, SMACH, [14]. It is intended to provide rapid engineering level analysis for aerothermal heating, aerodynamics and material response including shape change.

Numerical rebuilding of the transonic tests will be performed by DLR using the TAU code [21]. At transonic speed the flow in the base region has a significant influence on the aerodynamic coefficients, therefore, static coefficients will be computed with and without sting for different shapes and Mach numbers in order to extract the impact of the sting first.

#### 4. LOW TEMPERATURE ABLATOR AND MODELS

The behavior of an ablator during planetary entry is a complex physical process, which is strongly related to the flight environment, i.e. the flow enthalpy, the stagnation pressure and the heat flux. Ground-based wind tunnel facilities cannot completely duplicate these conditions. Therefore, low-temperature ablation experiments in cold blow-down wind tunnels are an option to mimic certain aspects and will be the focus of the present study.

To realize a shape change in low-enthalpy conditions, materials can be used which melt, i.e. exhibit a phase change from solid to fluid, under the test conditions, i.e. [7], [8], [2], [6]. Initial pre-tests, prior to the start of the activities within the TRP, were performed with stearin, which is an excellent candidate for pure melting materials, due to its low melting temperature of approx. 337K. The manufacturing of models is rather straight forward.

However, ablative heat shields of ERC ideally sublime from solid to gas phase [1], which is why it is reasonable to use low-temperature subliming materials for low-enthalpy tests in hypersonic wind tunnels. Five possible material candidates were considered: dry ice (CO<sub>2</sub>), naphthalene (C<sub>10</sub>H<sub>8</sub>), camphor (C<sub>10</sub>H<sub>16</sub>O), dichlorobenzene (C<sub>6</sub>H<sub>4</sub>Cl<sub>2</sub>), ammonium chloride (NH<sub>4</sub>Cl). They feature inexpensive,

easily moulded and non-toxic characteristics [1]. Additionally, their products of ablation are chemically simple and non-reactive, except for ammonium chloride [6]. The latter dissociates upon heating into ammonia and acid hydrogen chloride which can lead to corrosion in the experimental facility and is therefore discarded. Moreover, all sublimers, except for dry ice, are solid under atmospheric conditions and their triple point pressures lie below one atmosphere. Thermal properties regarding sublimation behavior of several materials are shown in Table 2.

**Table 2: Properties of several low-temperature subliming material candidates [1] [11] [5] [10]**

Material	$\Delta H_s$ [kJ/kg]	M [g/mol]	$T_{tr}$ [K]	$P_{tr}$ [kPa]
Dry Ice (CO <sub>2</sub> )	576.8	44	217	518.0
Naphthalene (C <sub>10</sub> H <sub>8</sub> )	577.8	128	353	1.0
Camphor (C <sub>10</sub> H <sub>16</sub> O)	244.9	152	453	51.4
Dichlorobenzene (C <sub>6</sub> H <sub>4</sub> Cl <sub>2</sub> )	493.1	147	326	1.3

All materials, shown in Table 2 were examined whether they experience a phase change from solid to gas in the range of H2K test conditions. Figure 4 shows their triple points, as well as selected sublimation lines from [5], in a T-p-diagram. In addition, stagnation temperature and pressure combinations for all considered H2K conditions are included (Table 1). The pressure corresponds to the stagnation pressure after a steady adiabatic normal shock (pressure coefficient of  $c_p \sim 1.8$ ). The corresponding temperatures represent the recovery temperature with the assumption of a laminar recovery factor of  $r = \sqrt{Pr} = \sqrt{0.72}$ . Both, the stagnation pressures and recovery temperatures, can only act as a first estimate to characterize the phase conditions of the coating in the actual tests, since the vapor pressure of the sublimated phase of the coating above the solid as well as the wall temperature based on the mass and energy balance need to be taken into account. This is addressed later in this chapter.

As a first step for identification of suitable LTA materials at H2K conditions, the triple point pressure lines of the LTA candidates are investigated. In Figure 4, it is visible that the triple point pressure of naphthalene and dichlorobenzene is below the possible test conditions. Therefore, they would melt rather than sublime. Carbon dioxide fulfils by far this requirement with its high pressure and low temperature of the triple point. But the manufacturing and storing without sublimation under atmospheric conditions is challenging due

to its very low triple point temperature below atmospheric conditions. Finally, camphor seems a good choice as sublimator in H2K, since the stagnation pressures can be designed to lie below the triple point pressure and the triple point temperature is low enough to be overcome in wind tunnel conditions but high enough to be above atmospheric standard conditions. However, some amount of camphor also sublimates at ambient conditions due to the inherent large vapor pressure, but it is manageable with a suitable handling. Based on the above analysis, stearin was chosen as melting material and camphor as sublimating material for this TRP.

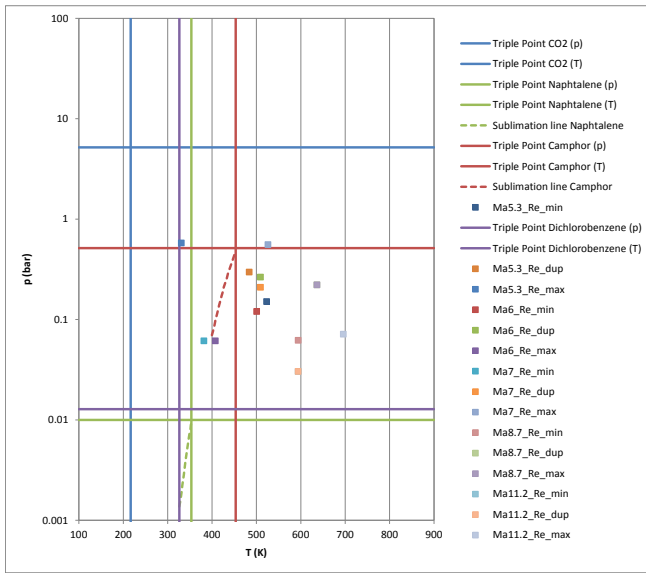


**Figure 4: Triple point pressure and temperature of different low-temperature sublimating materials relative to surface pressures and recovery temperatures at test conditions of H2K flow envelope**

For the preliminary pre-tests, the mass flow rate of the sublimated camphor was approximated with a method according to Baker [16] and Kubota [17]. They derived an iterative solution to the mass and heat conservation equations for the case of vaporization into a boundary layer, with the assumption of a binary system of vapor and air without chemistry, a Prandtl and Lewis number of unity, steady state conduction and ignoring influences of radiative heating. Figure 5 contains a map of possible blowing parameters  $B' = \frac{\dot{m}}{\rho_e V_e St_{blow}}$ , depending on the corresponding wall temperatures, at the wall. The parameter includes the mass flow rate of camphor  $\dot{m}$ , the fluid density  $\rho_e$  and velocity  $V_e$  at the boundary layer edge and the Stanton number  $St_{blow}$  including an approximation for the reduction by the blowing ratio of camphor [16]. For the calculations

the material properties listed in Table 2 were used, except of the heat of sublimation, which was used with 351.9kJ/kg according to [16]. In the figure the general trend is visible with an increasing blowing parameter with increasing stagnation temperature  $T_0$  (numbers given horizontally) and decreasing stagnation pressures i.e. pressures at the boundary layer edge (both given as numbers vertically with the stagnation pressures in brackets).

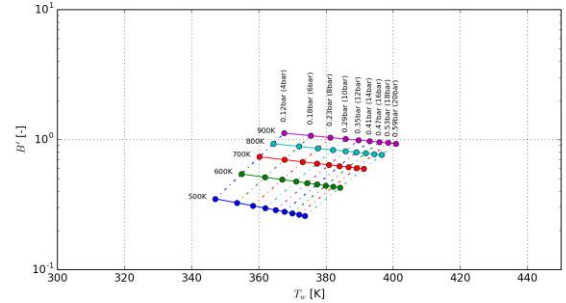


**Figure 5: Blowing parameters for the H2K Mach 6 envelope and camphor**

Another general challenge of LTA materials is the fabrication of wind tunnel models. Common methods of model fabrication are casting or cutting techniques [1], [5], [6], [9]. A further fabrication technique is sintering as described in [5]. This technique usually compresses the raw material powder at different rates of pressures either directly in a mould with the negative of the final OML shape or first in a separate generic geometry and then introduced in a mould with a piston. The finished models are described as strong, devoid of visible crystalline structure and easily manufacturable, despite some problems of model integrity during testing [5]. For this TRP, a sintering technique was chosen. The main strategy for both liquefying (stearin) or sublimating (camphor) coating material is a solid, metallic model core to ensure model integrity during/after material recession and to ensure a high precision interface to the force balance (Figure 6). The metallic model core acts as the piston with a defined offset of 5mm from the final OML. The offset was derived based on the numerical predictions of FGE. The powder of the LTA is inserted in a suitable mould with the negative shape of the final OML.

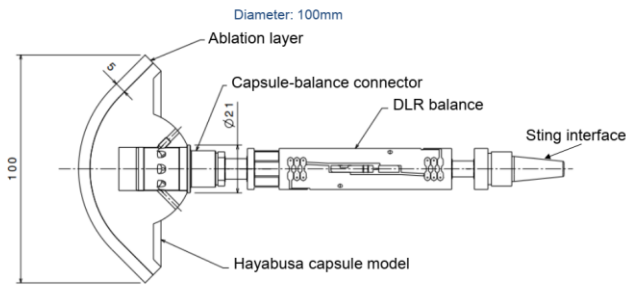


**Figure 6: Schematic of the H2K model and balance**

Depending on the applied pressures, the resulting texture of the coating is smooth, either made of a clear, translucent mass or a milky white, opaque mass. Both appearances are already known from previous investigations in [5], which described both material variants to occur and both variants showed the same behavior in a static oven and wind tunnel tests. Examples of the resulting coating in this TRP are visualized in Figure 7. To characterize the camphor coating, additional pycnometer measurements were applied to derive the solid density. Samples were cut off the capsule after sintering from two different regions, i.e. the nose and the conical region. Typical densities of  $899 \text{ kg/m}^3$  at the nose and  $861 \text{ kg/m}^3$  at the cone region were derived, if a milky white, opaque mass was targeted. This is lower compared to the literature value of  $990 \text{ kg/m}^3$  and can be most likely attributed to small voids within the material, giving it its appearance. If higher sintering pressures are used, typical densities of  $953 \text{ kg/m}^3$  at the nose and  $937 \text{ kg/m}^3$  at the cone region were measured. Besides the density, it is evaluated to characterize further material parameters.



**Figure 7: H2K wind tunnel models with LTA coating**

The OML of the resulting shapes after sintering were measured via the tactile Carl Zeiss Prismo device as well as the optical 3D-profilometer and compared to the reference CAD geometry. From initial versions with typical deviations of the order of 1mm an optimized sintering procedure lead to typical rms deviations of approx. 0.1mm at the nose and approx. 0.6mm at the cone. The resulting diameter differed by less than 0.2%. An image of the axial deviation from the CAD geometry  $\Delta z$  is shown in Figure 8. The procedure is

further optimized to reduce the cone deviations and the resulting surface roughness.

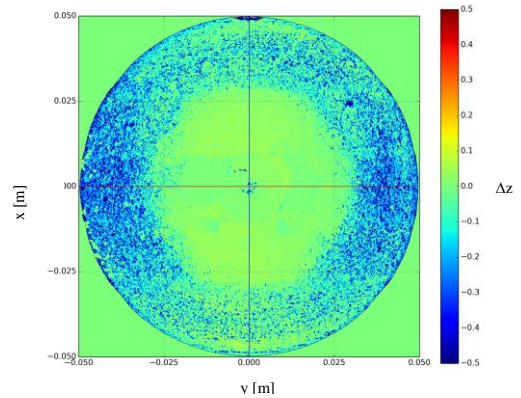


**Figure 8: LTA OML measurements**

## 5. PRE-TESTS

Selected pre-tests were performed to check the camphor coating behavior, the balance integrity, the IR camera output and in-situ recession measurements (Schlieren method). At the time of the pre-tests, not all of the necessary equipment for the PTSV was available, therefore no data is shown yet. The inflow condition used was the minimum Reynolds number condition at Mach 6 (see Table 1). Figure 9, a shows a Schlieren image and Figure 9, b shows an IR image during testing. The Schlieren image shows clearly the bow shock in front of the capsule, as well as the expansion around the shoulders. The model contour is clearly visible and the Schlieren data was used to extract the stagnation point recession over the test time of 20s, as described in chapter 3, which resulted in  $s = 0.65 \pm 0.16 \text{ mm}$ . The stated uncertainty results from an approximated reading uncertainty of one pixel. The final set-up is planned to have a higher resolution to lower this uncertainty. The IR image of Figure 9, b shows with red areas the hotter stagnation region compared to the slightly cooler cone regions. The surface temperature reached a nearly constant stagnation point value of approx.  $T_w = 85 \text{ }^\circ\text{C}$  (assuming a constant emissivity for camphor of 0.94, as given by several IR camera provider) where 90% of this value is reached after  $t_{T90} \approx 4.5 \text{ s}$ .

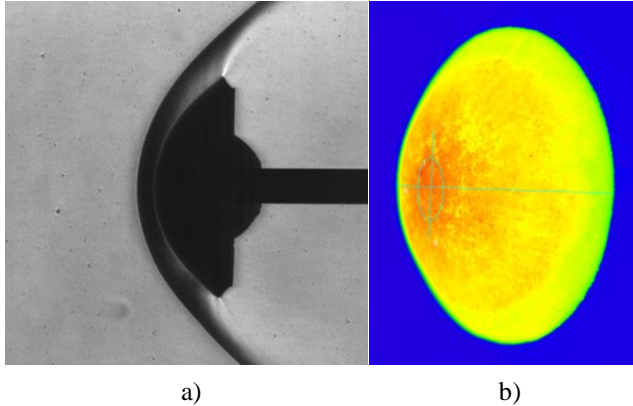


**Figure 9: Pre-test Schlieren image a) and IR image b)**

The model was weighted prior and after the test which resulted in a difference of 7.8g of evaporated camphor material. An approximate representative total recession may be derived from this value, if it is assumed that the camphor material with a literature density of  $990\text{kg/m}^3$  evaporated evenly and parallel to the initial OML. Under these assumptions a recession of  $0.73\pm 0.08\text{mm}$  would result, where the uncertainty stems from a density variation of  $\pm 10\%$ . This value is consistent with the value derived by the Schlieren method, if the uncertainties are considered. However, it is expected that the recession in the stagnation region is different compared to the cone region, which violates the evenly distributed recession assumption.

The binary mixture approach according to Baker is used to estimate the surface temperature and recession, assuming either equilibrium between the solid and vapor phase or assuming non-equilibrium [16]. The latter is assumed to be more realistic, since an equilibrium condition is usually not reached within a boundary layer flow with convective and diffusive transport of the vapor. A cold wall stagnation heat flux according to the method of Fay and Riddell [4] with an equivalent radius of  $R_{N, \text{equ}} = 57.3\text{mm}$  of  $40.1\text{kW/m}^2$  at a stagnation pressure of  $p_{\text{stag}} = 0.119\text{bar}$  was used. This resulted with an equilibrium assumption in a recession rate of  $0.027\text{mm/s}$ , which in turn result in a total recession of  $0.54\text{mm}$  after 20s test time. With a non-equilibrium assumption the values only slightly change to a recession rate of  $0.026\text{mm/s}$ , which would result in  $0.53\text{mm}$  after 20s test time. For the non-equilibrium case, the method result in an iterated wall temperature of  $T_w = 85.9^\circ\text{C}$ . Both, the wall temperature as the total recession are very close to the experimentally observed values.

## 6. SUMMARY AND OUTLOOK

The TRP MODSHAPE addresses the impact of a shape change of a planetary entry probe due to recession on the

aerodynamic stability. This paper described the planned strategy to fulfil this goal with experimental and numerical efforts.

For tests in the hypersonic wind tunnel H2K, stearin as liquefying and camphor as sublimating LTA coating material were chosen, based on preliminary analyses of suitable inflow and corresponding phase change conditions. Two different inflow conditions at Mach 6 and specific model scaling were selected as tradeoff between counteracting requirements from the aerothermodynamic and aerodynamic flow duplication and measurement constraints. To measure the shape change in-situ, an optical stereophotogrammetry set-up will be used together with a technique based on Schlieren images. The aerodynamic measurements will be performed with an internal six-component balance. Preliminary tests showed that the general set-up and model coating do behave as expected and data from IR and Schlieren recession measurements are consistent and are in agreement with preliminary approximations.

The next steps include the actual in-situ recession and aerodynamic measurement test campaign in the hypersonic wind tunnel H2K. This is followed by the test campaign with fixed shape-modified models in the trans- to supersonic regime. Together with CFD support, a static aerodynamic database will be created, which will be used to analyze the shape change impact on flight quality and dynamic attitude behavior, performed by TAS-I. With valid aerodynamic data for the case of asymmetric shape change, the effect of the resulting trim moment on the stability of the capsule can be analyzed. This will enable a better estimate, if it is conservative to include shape change in ERC dynamics. Furthermore, it is planned to perform an assessment of the shape change impact on the forebody pressure distribution, and with that, on attitude reconstructions using surface pressures, according to [22],[23].

## 7. ACKNOWLEDGMENT

This work was performed under ESA contract 4000122733/17/NL/KML.

## 8. REFERENCES

- [1] Callaway, David W., "Photogrammetric Measurement of Recession Rates of Low Temperature Ablators in Supersonic Flow," Dissertation, Air Force Institute of Technology, Air University, Air Education and Training Command, Georgia, 2003
- [2] Williams, E. P. "Experimental studies of ablation surface patterns and resulting roll torques." AIAA Journal 9.7 (1971): 1315-1321.

- [3] Callaway, D. W., et al. "Ablation Measurements and Analysis of Solid Carbon Dioxide Models at Mach 3." *Journal of Spacecraft and Rockets* 51.1 (2014): 213-225.
- [4] Fay, James A. "Theory of stagnation point heat transfer in dissociated air." *Journal of the Aerospace Sciences* 25.2 (1958): 73-85.
- [5] Charwat, Andrew F. Exploratory studies on the sublimation of slender camphor and naphthalene models in a supersonic wind-tunnel. No. RAND/RM-5506-ARPA. RAND CORP SANTA MONICA CA, 1968.
- [6] Lipfert, Fred, and John Genovese. "An experimental study of the boundary layers on low-temperature subliming ablators." *AIAA Journal* 9.7 (1971): 1330-1337.
- [7] Ginoux, J. J., and H. W. Stock. "Experimental results on crosshatched ablation patterns." *AIAA Journal* 9.5 (1971): 971-973.
- [8] Stock, Hans W., and M. Goddard. Cross-hatching: A comparison between behaviour of liquifying and subliming ablation materials. Von Karman Institute for Fluid Dynamics, 1973.
- [9] Combs, Christopher S., Noel T. Clemens, and Paul M. Danehy. "Visualization of capsule reentry vehicle heat shield ablation using naphthalene PLIF." (2014).
- [10] Rohac, Vladislav, et al. "Recommended vapour and sublimation pressures and related thermal data for chlorobenzenes." *Fluid Phase Equilibria* 157 (1999): 121-142.
- [11] Kohlman, David L., and Richard W. Richardson. "Experiments on the use of dry ice ablating wind-tunnel models." *Journal of Spacecraft and Rockets* 6.9 (1969): 1061-1063.
- [12] Ferri, A., Pelle, S., Belluco, M., Voirin, T., & Gelmi, R. (2018). The exploration of PHOBOS: Design of a Sample Return mission. *Advances in Space Research*, 62(8), 2163-2173.
- [13] Sancho, J., Rebolo, R., Neeb, D., EFFECT OF ABLATION SHAPE CHANGE IN TRANSONIC AND SUBSONIC AERODYNAMICS FOR A HIGH SPEED ENTRY CAPSULE, FAR conference 2019.
- [14] Lingard et al.; Supersonic Parachute Testing using a Maxus Sounding Rocket Piggyback Payload. 8th European Symposium on Aerothermodynamics for space Vehicles, ESA SP-636-91729, 2015.
- [15] Konolige, Kurt. "Projected texture stereo." 2010 IEEE International Conference on Robotics and Automation. IEEE, 2010.
- [16] BAKER, R. "Low temperature ablator nosetip shape change at angle of attack." 10th Aerospace Sciences Meeting. 1972.
- [17] Kubota, Toshi. "Ablation with Ice Model at M= 5.8." *ARS Journal* 30.12 (1960): 1164-1169.
- [18] Preci, A., Gülhan, A., Clopeau, E., Tran, P., Ferracina, L., & Marraffa, L. (2016). Dynamic characteristics of MarcoPolo-R Entry Capsule in low subsonic flow. *CEAS Space Journal*, 8(1), 23-33.
- [19] Barraclough, S., Ratcliffe, A., Buchwald, R., Scheer, H., Chapuy, M., Garland, M., & Rebuffat, D. (2014, June). Photoprint: a European phobos sample return mission. In 11th International Planetary Probe Workshop (Vol. 1795).
- [20] Seiff, A., Venkatapathy, E., Haas, B., & Intrieri, P. (1996). Galileo probe aerodynamics. In 14th Applied Aerodynamics Conference (p. 2451).
- [21] Fertig, Markus, Dominik Neeb, and Ali Gülhan. "Windtunnel Rebuilding and Extrapolation to Flight at Transsonic Speed for ExoMars." 7th European Symposium on Aerothermodynamics. Vol. 692. 2011.
- [22] Van Hove, Bart, et al. "ExoMars Flush Air Data System: Entry Simulation and Atmospheric Reconstruction Method." *Journal of Spacecraft and Rockets* (2019): 1-16.
- [23] Schleutker, Thorn, et al. "ExoMars Flush Air Data System: Experimental and Numerical Investigation." *Journal of Spacecraft and Rockets* (2019): 1-12.
- [24] Gawehn, Thomas and Neeb, Dominik and Tarfeld, Frank and Gülhan, Ali and Dormieux, M. and Binetti, P. and Walloschek, T. (2011) Experimental investigation of the influence of the flow structure on the aerodynamic coefficients of the IXV vehicle. *Shock Waves*, 21 (3), pp. 253-266. Springer. DOI: 10.1007/s00193-011-0326-y.
- [25] Brazier, Jean-Philippe and Martinez Schramm, Jan and Paris, Sébastien and Gawehn, Thomas and Reimann, Bodo (2016) An overview of HyFIE Technical Research Project: cross-testing in main European hypersonic wind tunnels on EXPERT body. *CEAS Space Journal*, 8 (3), pp. 167-176. Springer. DOI: DOI 10.1007/s12567-016-0117-5 ISSN 1868-2502.
- [26] Tran, Philippe, and James Beck. "EXOMARS Entry Demonstrator Module aerodynamics." 7th European Symposium on Aerothermodynamics. Vol. 692. 2011.
- [27] IDS Ensenso system description, [https://de.ids-imaging.com/tl\\_files/img/landingpage/ensenso\\_landingpage/Ensenso%20Operating/ensenso-3d-camera-projection.png](https://de.ids-imaging.com/tl_files/img/landingpage/ensenso_landingpage/Ensenso%20Operating/ensenso-3d-camera-projection.png)